Biochimica et Biophysica Acta, 1100 (1992) 207–215

BBABIO 43606

Spectroscopic characterization of photoinhibited Photosystem II and kinetic resolution of the triggering of the D_1 reaction center protein for degradation

Klaas J. van Wijk [1], Bertil Andersson and Stenbjörn Styring

Department of Biochemistry, Arrhenius Laboratories for Natural Sciences, Stockholm University, Stockholm (Sweden)

(Received 4 December 1991)

Key words: D_1-protein degradation; EPR; Electron transport; Low temperature; Photoinhibition; Photosystem II

Photoinhibition of isolated thylakoids results in inactivation of Photosystem II electron transport and proteolysis of the D_1 reaction center protein. At low, non-freezing temperatures the mechanism of inactivation for Photosystem II electron transport can be experimentally studied without interference of secondary damaging effects, since the degradation of the D_1-protein does not occur. Here we have applied electron paramagnetic resonance (EPR) spectroscopy to characterize the sequential events leading to inhibition of PS II electron transport and triggering of the D_1-protein for degradation at 2°C. Two principle kinetics of inactivation and damage were observed: (i) inactivation with a half-time of 1 to 1.5 h in case of steady-state electron transport through Photosystem II, the induction of the S_2-state multiline EPR signal, the EPR signal from Q_A-Fe^{2+} and lowering of the F_v/F_m fluorescence ratio. This is explained by over-reduction of the first quinone acceptor (Q_A) leading to impairment of its function. (ii) Inhibition with a half-time of 3–4 h in case of EPR Signal II_{slow}: inhibition of the primary charge separation reaction and release of manganese from its site in the oxygen evolving system. We were also able, for the first time, to follow the kinetics for the triggering of the D_1-protein for degradation. This triggering followed the slower kinetic phase and is likely to be the result of conformational changes in the protein induced by the highly reactive singlet oxygen. Additionally, a dark-stable cationic radical with $g = 2.0031$ and 10–11 G wide was progressively induced during the inhibition and was tentatively attributed to a carotenoid cation.

Introduction

Strong illumination of the photosynthetic apparatus leads to inactivation of the electron transfer through Photosystem II (PS II) and subsequently to breakdown of the D_1-reaction center protein (for reviews: see Refs. 1–4). PS II is repaired through synthesis and incorporation of new D_1-protein into the complex. Two principal mechanisms for this photoinhibition have been proposed: inactivation of electron transport through overreduction of the quinones at the acceptor side of PS II, leading to an oxygen dependent protein degradation or inactivation through cationic radicals at the donor side of PS II leading to an oxygen independent degradation of the D_1-protein (see Ref. 4 and references therein).

The actual degradation of the D_1-protein is catalyzed by one or more proteolytic enzymes located in the PS II complex [5,6] and can be inhibited by inhibitors specific to serine-type proteinases [7,8]. The proteolytic nature of the D_1-protein degradation can also be demonstrated by subjecting isolated thylakoids to photoinhibitory illumination at 2°C [9]. This leads to a loss of electron transport activity of PS II, as measured by the Hill-reaction, but not to any significant loss of the D_1 protein. However, when the temperature is raised above 7–10°C, the D_1-protein is degraded

[1] Present address: Department of Plant Biology, University of Groningen, P.O. Box 14, 9750 AA Haren, The Netherlands.

Abbreviations: Chl, chlorophyll *a*; DAD, 3,6-diamino-durol; DCIP, 2,6-dichlorophenolindophenol; DPC, 2,2′-diphenylcarbonic dihydrazide; F_0, basic fluorescence; F_m, maximum fluorescence; F_v, variable fluorescence; PS II, Photosystem II; P680, the primary electron donor of PS II; Pheo, pheophytin – the primary electron acceptor of PS II; PpBQ, phenyl-*para*-benzoquinone; Q_A, the first quinone acceptor of PS II; Q_B, the second quinone acceptor of PS II; Signal II_{slow}, EPR signal from the oxidized Tyr_D, accessory electron donor on the D_2-protein; Tyr_Z, tyrosine residue, acting as electron carrier between P680 and the water oxidizing system.

Correspondence: S. Styring, Department of Biochemistry, Arrhenius Laboratories for Natural Sciences, Stockholm University, S-106 91 Stockholm, Sweden.

even in complete darkness [9]. Thus, during the high light treatment the D_1-protein is damaged as a consequence of the photoinactivation. It thereby becomes 'triggered' for degradation, but the actual degradation can only take place at higher temperatures.

Thus, PS II photoinhibited at low temperatures should provide an excellent system to experimentally resolve the light-induced inactivation of PS II from the protein degradation. This is of crucial importance since in previous studies of the mechanisms of photoinhibition these two events have been overlapping.

With the combination of electron transport measurements, EPR spectroscopy and quantitative protein analysis of isolated PS II membranes photoinhibited at low temperatures we have kinetically resolved several sequential steps during the photoinactivation of the electron transport and triggering of the D_1-protein for degradation. Furthermore, we report the progressive formation of an unidentified dark stable cationic radical in PS II.

Materials and Methods

Preparation of photosynthetic materials

PS II enriched membranes were prepared as in Ref. 10 with the modifications in Ref. 11. The PS II enriched membranes were suspended to 4–5 mg chlorophyll ml^{-1} in 20 mM Mes-NaOH (pH 6.3), 15 mM NaCl, 5 mM $MgCl_2$ and 0.4 M sucrose and stored in liquid nitrogen.

Photoinhibition treatment and sample preparation

PS II enriched membranes, suspended in a volume of 10 ml at a concentration of 175 μg Chl ml^{-1}, were under constant slow stirring, illuminated with heat filtered white light (3500–4000 $\mu E/m^2$ per s). During the illumination, the suspension was thermostated at 0–4°C. Control samples were handled in identical manner, with the exception that they were kept in darkness or in very low light (1–10 $\mu E\ m^{-2}$ per s). For studies on the D_1-protein degradation the preilluminated samples were kept for 2 h at room temperature in the dark.

Control and photoinhibited samples intended for EPR measurements were concentrated by two centrifugations at 10000 rpm for 1 min at 1°C. The pellet was resuspended in ice-cold buffer and immediately transferred to calibrated EPR tubes (approx. 3 mg Chl ml^{-1}) and stored in liquid nitrogen. From all the EPR samples, aliquots for electron transport measurements and D_1-protein analysis were taken immediately before freezing to allow direct comparison with the measured EPR characteristics.

The total manganese content of the PS II enriched membranes was determined by room temperature EPR spectroscopy of acidified samples. The suspensions were spun down, and the pellet was acidified with H_2SO_4 (final concentration 1 M) to release the manganese. Calibration was done by addition of known amounts of $MnCl_2$.

Electron transport and chlorophyll fluorescence measurements

PS II electron transport at 20°C in saturating light was measured polarographically as O_2-evolution in the presence of 0.2 mM PpBQ or spectroscopically in the presence of 50 μM DCIP in absence or presence of the artificial electron donor DPC (1 mM).

Steady state chlorophyll fluorescence was measured using a pulse amplitude modulation fluorometer (PAM 101, Walz, Effeltrich, Germany). Basic fluorescence (F_0) was measured with the measuring beam at 1.6 kHz. Maximal fluorescence (F_{max}) was measured by giving a saturating light-pulse (1–3 s) [12].

EPR spectroscopy

X-band low-temperature and room temperature EPR spectra were recorded at respectively 9.239 GHz and 9.77 GHz microwave frequency with a Bruker ESP 300 spectrometer equipped with an Oxford instruments He-cryostat. Normalization of the EPR spectra for chlorophyll content and tube-diameter were done with the ESP300 program. EPR conditions for the measured signals are indicated in respective figure legends.

In measurements of the EPR signal from Q_A^--Fe^{2+}, formate was added to a final concentration of 25 mM in order to enhance the signal amplitude [13]. Q_A was chemically reduced by 50 mM dithionite or by illumination at 77 K. To avoid degradation of triggered D_1-protein, the incubations with formate and/or dithionite were performed on ice and in darkness for 30–40 min, which was found to be saturating at this temperature. For measurements of the total amount of photoreducible pheophytin, diluted samples (approx. 1 mg Chl ml^{-1}) were illuminated for 6 min at 20°C (saturating at this concentration) after the addition of dithionite to a final concentration of 50 mM [14] and dark incubation for 40 min on ice. The short time for the photoaccumulation illumination was chosen to minimize D_1-protein degradation.

The spin-polarized chlorophyll triplet EPR signal from ^{3}P680 was measured during continuous illumination in the EPR cavity at 4 K. Prior to the measurements the samples were made anaerobic by careful bubbling with argon for at least 10 min. This argon-flush was included to allow observation of the spin-polarized triplet signal (if formed) in the samples that contain oxygen due to the sample preparation protocol. Otherwise, the oxygen would quench any triplet formed which might lead to erranous interpretation of the results (Vass and Styring, unpublished data).

Quantification of Signal II_{slow} and the radical around $g = 2.003$ were done by double integration using the ESP300 software.

Protein analysis

Protein analysis was carried out by sodium dodecyl sulfate polyacrylamide gel electrophoresis, as previously described [15]. The 22 kDa protein in PS II was used as an internal standard since it is normally not degraded during photoinhibition [9]. Western blotting using monospecific antibodies against the D_1- and 22 kDa proteins, was performed essentially according to Ref. 16 using ^{125}I-labelled protein A for detection. For quantification, the autoradiograms were scanned by a laser densitometer.

Chlorophyll was measured in 80% aceton according to Arnon [17].

Results

Steady state electron transport

PS II electron transport was measured in all samples in order to cross-correlate the photoinactivation with the various measured PS II parameters. Inhibition of the steady state oxygen evolution, by strong illumination at 2°C, occurred with an approximate half-time of 1 h (Fig. 1). The inhibition of the electron transport in the presence of the artificial electron donor DPC was somewhat slower and occurred with a half time of approx. 1.5 h (Fig. 2). In the dark control samples there was no reduction of the steady-state electron transport rates after 3 h incubation at 2°C.

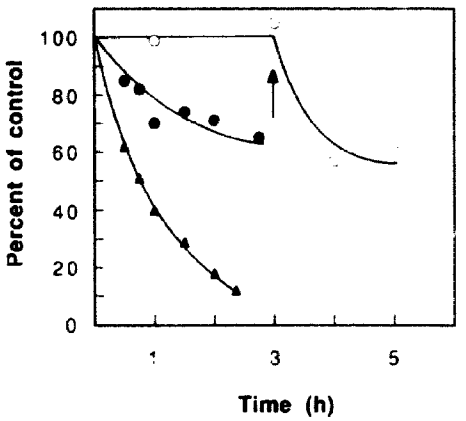

Fig. 1. Changes in the content of the D_1 reaction center protein in PS II during photoinhibitory illumination at 2°C and subsequent room-temperature incubation in the dark. The arrow indicates the time for the transfer of the samples to room temperature in the dark. (○) D_1-protein content during illumination at 0–4°C and during a subsequent period at 20°C in the dark. The samples were illuminated for defined times before the protein measurement. (●) Amount of the D_1-protein 'triggered' for degradation during photoinhibition at 2°C. Each sample was illuminated for a defined time and then incubated for 2 h at 20°C in the dark before the protein measurement. (▲) Inhibition of the O_2-evolution during low-temperature illumination. The O_2 evolution in the non-inhibited samples was 420 μmol O_2 /mg Chl per h.

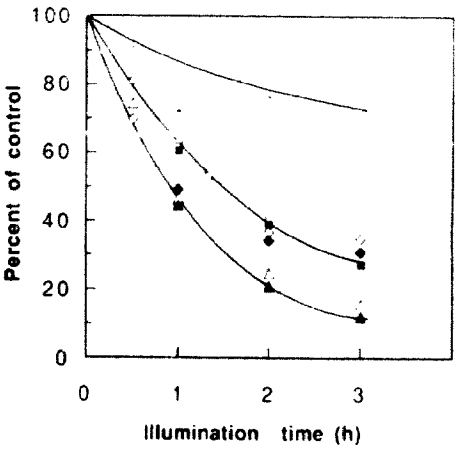

Fig. 2. Kinetics of the inhibition of the DCIP-reduction measured in presence (□, ■) or absence of DPC (△, ▲), the S_2-state multiline EPR signal (○, ◆) and EPR Signal II_{slow} (+). Open symbols indicate measurements immediately after the illumination, closed symbols indicate measurements after the illumination followed by 2 h dark incubation at room temperature. The size of the S_2-state multiline EPR signal was measured by the sum of six peaks [30]. The amplitude of Signal II_{slow} was measured at the low field maximum (see Fig. 4). EPR conditions for the S_2-state multiline EPR signal: temperature 10 K; microwave power 20 mW; modulation amplitude 25 G. EPR conditions for Signal II_{slow}: temperature 15 K; microwave power 0.49 μW; modulation amplitude 3.2 G.

The D_1 reaction center protein and its triggering for degradation

During the strong illumination at low temperature no or very little degradation of the D_1-protein occurred (Fig. 1) in contrast to what is seen at room temperature. However, when the photoinactivated PS II membranes were transferred to 20°C and subsequently incubated in darkness, the D_1-protein was degraded (Fig. 1) in accordance with recent studies on thylakoid membranes [9]. Thus, the strong illumination at 2°C induced a population of inhibited PS II centers with the D_1-protein trapped in a state triggered for degradation. Once transferred to 20°C, the triggered D_1-protein was degraded with a half time of about 15 min (not shown).

We were also able to measure the kinetics for the triggering of the D_1 protein. This was done in an experiment where the D_1 protein content was measured in samples illuminated for various periods of time at 2°C and then subsequently incubated for 2 h at 20°C. The experiment revealed a time-dependent increase in the fraction of the D_1-protein that was degraded during the room temperature incubation (Fig. 1). This fraction represents the D_1-protein that was

triggered for degradation during the strong illumination at 2°C and amounted to 30–40% of the D_1 protein after 3 h photoinhibition. The triggering of the D_1-protein occurred with a half-time of 3–4 h (Fig. 1).

Fig. 1 also compares the extent of D_1-protein triggering and the inhibition of electron transport. The PS II electron transport inhibition preceeded the triggering of the D_1-protein as expected from earlier measurements of D_1-protein degradation [9,15].

Manganese binding

As shown in Fig. 3, manganese was released from the PS II membranes during the strong illumination at the low temperatures. The Mn-release was significantly slower than the loss of the oxygen evolution (Fig. 3). After 3 h of photoinhibitory illumination, 35% of the manganese was lost. Interestingly, the Mn-release correlates closely to the amount of the D_1-protein that was triggered for degradation (Fig. 1) which indicates that the manganese was released prior to the actual degradation of the D_1-protein.

Effects on the S_2-state multiline EPR signal

The multiline signal, which is detectable in PS II centers in the S_2-state [18], is an indication of the structural and functional intactness of the manganese cluster. In well dark-adapted PS II, most of the centers are in the S_1-state and illumination at 198 K induces the S_2-state multiline signal if Q_A is able to accept one electron. As a consequence of photoinhibition at 2°C, the induction of the S_2-state multiline signal at 198 K was inhibited with nearly identical kinetics as the steady-state electron transport rate in presence of DPC and thus somewhat slower than the loss of steady state oxygen evolution (Fig. 2). No S_2-state multiline EPR signal could be observed in the inhibited samples before illumination at 198 K.

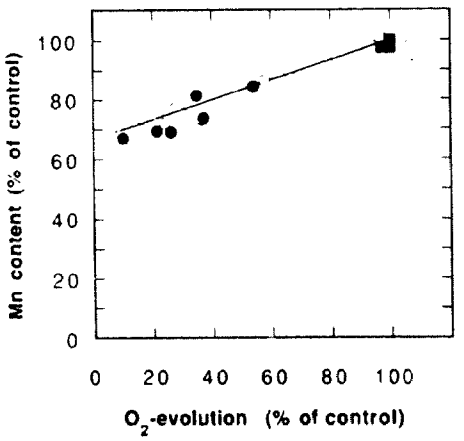

Fig. 3. Correlation between the content of bound manganese in the PS II enriched membranes, immediately after the strong illumination (○) or after a subsequent 2 h dark incubation at room temperature (●) and the inhibition of the O_2-evolution. The manganese content was normalised to the sample concentration and is expressed in % of the manganese in the non-photoinhibited control. The 100% value represents 1 Mn^{2+} per 71 (±1.7) chlorophyll $a + b$ ($n = 8$). (□, ■) represent non-illuminated samples kept for 3 h at 2°C (open symbols) or 3 h at 2°C followed by 2 h incubation at room temperature (closed symbols).

EPR Signal II_{slow}

Signal II_{slow} originates from a dark stable oxidized tyrosine radical on the D_2-protein [19,20]. During the photoinhibitory illumination at 2°C, the amplitude of Signal II_{slow} was progressively decreased (Fig. 2) resulting in a loss of approximately 30% of the signal after 3 h. The decrease was irreversible since the lost signal could not be regained by illumination. The decrease in the amplitude of Signal II_{slow} was slower than the inhibition of the DCIP-reduction rate or the S_2-state multiline signal (Fig. 2). Instead it correlated with the release of manganese and the triggering of the D_1-protein for degradation.

Induction of a cationic radical

Notably, overlaying the decreasing Signal II_{slow} spectrum, the photoinhibitory treatment at low temperatures progressively induced a new radical signal (Fig. 4). This resulted in a relative increase of the high field maximum (3287 G) compared to the low field maximum (3281 G) (Fig 4; compare 0 h and 3 h spectra). Subtraction of Signal II_{slow} from the inhibited spectra, after normalization at the low-field maximum shows that the new radical is 10 ± 0.5 Gauss wide, with a g-value of $g = 2.0031 \pm 0.0001$ (Fig. 4; spectrum a). The radical increased in size during illumination and after 3 h illumination the size of the radical (estimated on basis of Signal II_{slow} in a dark control) was 0.16 spins per PS II reaction center initially present (Fig. 4, inset). The size of the radical is approximately correlated to the difference in inhibition in electron transport in the presence and absence of the electron donor DPC (Fig. 2). Although of somewhat similar magnitude, the induction of the radical is clearly slower than the triggering of the D1 protein for degradation.

This new radical was quite stable in the dark and 2 h dark incubation at room temperature decreased its amplitude by approx. 50% (Fig. 4, inset). We assign the new spectrum to a cationic radical since it could be reduced by ascorbate and dithionite (Fig. 4; spectrum b), while oxidants like PpBQ or ferricyanide had no effect on its spectrum.

The Q_A^--Fe^{2+} EPR signal

The bound quinone, Q_A, is EPR visible after single reduction, which is achieved experimentally by low-temperature illumination or in the dark by chemical reduction with dithionite. The EPR spectrum origi-

nates from magnetic interactions between the reduced Q_A and the acceptor-side iron [21]. Oxidized and double reduced forms of Q_A are EPR silent [18,22].

The ability to form the Q_A^--Fe^{2+} EPR signal was progressively lost during the photoinhibitory illumination at 2°C with a half-time of approx. 1.5 h (Fig. 5). No Q_A^--Fe^{2+} signal was observed in the inhibited centers prior to the reduction during the EPR experiment. This indicates that no significant fraction of stabilized Q_A^- was formed, in contrast to what has been experimentally observed during anaerobic photoinhibition [23]. The inhibition of the Q_A^--Fe^{2+} formation correlated with the loss of the DCIP-reduction in presence of DPC.

The primary charge separation reaction

The capacity to induce the primary radical pair $P680^+Pheo^-$, was measured by EPR after photoaccumulation of $Pheo^-$ in the presence of dithionite [14,18]. After 3 h of photoinhibitory illumination at 2°C approx. 45% of the inducible radical signal from $Pheo^-$ was lost (Fig. 5). The decrease of the signal occurred on the same time scale as the loss of Signal II_{slow}, the triggering for degradation of the D_1-protein and the release of manganese.

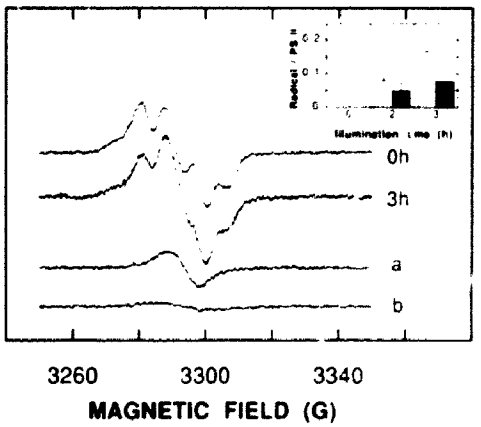

Fig. 4. The effect of photoinhibitory illumination on radical EPR spectra in PS II. The upper two spectra show the radical spectra after 0 and 3 h illumination. Before the strong illumination (0 h spectrum) the spectrum only contains Signal II_{slow}. After 3 h strong illumination the spectrum is a mixture of Signal II_{slow} and a radical spectrum. Spectrum a shows the spectrum of a 9–10 Gauss wide radical centered at $g = 2.0031$ which was induced during 3 h photoinhibition. The pure radical spectrum was obtained by subtraction of weighted amount of Signal II_{slow} from the 3 h spectrum. Incubation with 5 mM sodium ascorbate (5 mM) and the redox mediator DAD (2 mM) during 20 min reduced both the radical and Signal II_{slow} (spectrum b). Inset: induction of the radical after 2 and 3 h strong illumination at 2°C (unfilled stacks) and after a subsequent 2 h dark-incubation at room temperature (filled stacks). The size of the radical is expressed as spins per PS II. The bars indicate the standard error in the measurements ($n = 4$). EPR conditions: temperature 15 K; microwave power 0.49 μW; modulation amplitude 3.2 G.

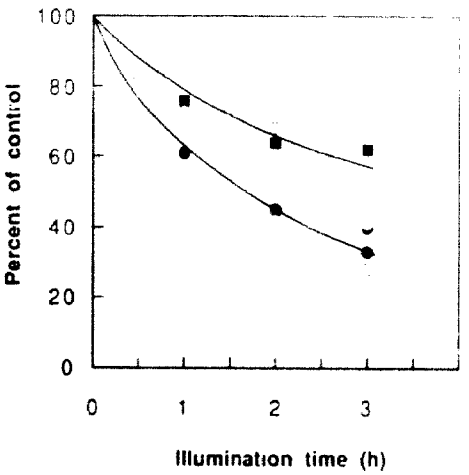

Fig. 5. Effect of photoinhibitory illumination on the EPR signals from Q_A and pheophytin $^-$. The Q_A-Fe^{2+} signal (○, ●) and the pheophytin $^-$ EPR signal (□, ■) were measured immediately after the illumination (open symbols) and after a subsequent 2 h dark period at 20°C (closed symbols). The amplitudes of the signals are expressed in percentage of the amplitudes in non-illuminated control samples. The Q_A-Fe^{2+} signal was developed in the samples by chemical reduction or illumination at 77 K. The pheophytin $^-$ radical signal was induced by photoaccumulation at 0°C under reducing conditions. Quantification of the Q_A-Fe^{2+} signal was done by measuring the amplitude of the peak at $g = 1.82$. Pheophytin $^-$ was quantified by double integration of the radical signal.

Spin polarized EPR signal from triplet P680

$^3P680$ originates from the recombination between $P680^+$ and $Pheo^-$ and is formed during illumination of PS II when Q_A is doubly reduced [22] or when the Q_A-site is empty [24]. $^3P680$ induced by illumination at 4 K gives rise to a spin polarised EPR signal. In addition, it was recently shown that photoinhibition under anaerobic conditions results in the accumulation of $^3P680$ forming centers due to stabilization of reduced Q_A species (both singly and doubly reduced) and subsequent loss of Q_A from its site (Ref. 23, Koivuniemi et al., unpublished data).

Therefore, we investigated whether our photoinhibited samples were also triplet forming. If any triplet formation was to be expected it should be found after prolonged photoinhibitory treatment, in centers which still had the capacity to photoaccumulate $Pheo^-$, but where no EPR visible Q_A could be induced. After 3 h, the population of such potential triplet forming PS II centers was about 15 to 20% of the total number of centers (Fig. 5). However, illumination of these photoinhibited samples at 4 K in the EPR cavity did not reveal any triplet formation. This indicates that triplet

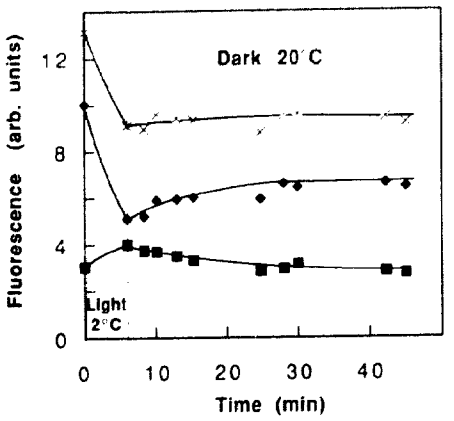

Fig. 6. Effect of 6 min strong illumination at low-temperature and subsequent dark incubation at room temperature on basic (F_0) (■), maximal (F_m) (×) and variable fluorescence (F_v) (◆). The first measuring point of F_0 after cessation of the strong illumination was taken after 25 s dark adaptation.

forming states either are quickly lost during photoinhibition in the presence of oxygen [23] or that the triplet yield is too low to be observed.

Chlorophyll fluorescence

During the first 10 min of photoinhibitory illumination at low temperature the dark fluorescence level, F_0, increased with approx. 10% (not shown) similar to what has been observed earlier (see for example Ref. 26). This most likely indicates the build-up of a small population of centers with stable forms of reduced Q_A [23,25,26]. During progressive photoinhibitory treatment, F_0 returned back to its initial value (not shown). In a separate experiment it was observed that the initial increase in F_0 was reversed by approx. 20 min dark incubation at room temperature (Fig. 6).

The ratio F_v/F_m decreased progressively during photoinhibition with the same kinetics as the inactivation of the O_2-evolution (not shown), similar to what was observed after low temperature photoinhibition in spinach [27] and in the cyanobacterium *Synechocystis* [25]. The lowering of F_{max} was always irreversible (Fig. 6).

Dark incubation at room temperature subsequent to photoinhibition at low temperature

The results presented above show that the major changes in the reducing properties of PS II during photoinhibition at low temperature occur prior to the D_1-protein degradation. We also applied the EPR-analyses to samples that were transferred to room temperature in the dark after termination of the photoinhibitory illumination. During this phase of the experiment, the D_1-protein degradation starts (Fig. 1) but no further inactivation of steady state electron transport occurs. In addition the EPR analysis revealed no further changes in the S_2-state multiline signal (Fig. 2), the Q_A-Fe^{2+} signal and the primary charge separation (Fig. 5). Moreover, there were no changes in the fluorescence characteristics.

Interestingly, there was no further release of manganese from the membranes during the D_1-protein degradation. This shows quite unexpectedly that all manganese from the inhibited reaction centers was released already in connection with the triggering of the D_1-protein for degradation. Earlier we correlated the Mn release with the D_1-protein degradation [15,28]. This apparent discrepancy results from the impossibility to kinetically discriminate between the triggering and the proteolysis of the D_1-protein in the earlier room-temperature experiments.

The remaining Signal II_{slow} decreased by 15 to 30% during dark incubation at room-temperature for 2 h in both the control and inhibited samples. This is normal during prolonged dark incubation and we ascribe this mainly to recombination with the S_0-state of the oxygen evolving system [29]. This fraction of the lost signal could be regained by illumination (not shown).

The amplitude of the new unidentified radical at $g = 2.0031$ decreased by approx. 50% during two the hours dark-incubation at room-temperature (Fig. 4; inset).

Discussion

In this report we have characterized the photoinactivation of PS II electron transport at low, non-freezing temperature where no proteolysis of the D_1-protein occurs. The experiments have therefore allowed resolution of the inhibition kinetics of the various partial reactions of PS II (Table I). In principle, the inhibitory events could be divided into two main categories that are summarized in Scheme I. Initially, with a half time for inactivation of 1 to 1.5 h there was a loss of the steady state electron transport both in absence and presence of the electron donor DPC, formation of the S_2-state multiline signal, induction of the EPR signal Q_A^--Fe^{2+} and lowering of the F_v/F_m fluorescence ratio. Thereafter, with a half time of 3–4 h, there was a loss of Signal II_{slow}, impairment of the primary charge separation capacity and release of the manganese from its binding site on the lumenal side of the PS II complex. With the same kinetics the D_1-protein was triggered for degradation. The actual degradation of the protein required transfer of the sample to 20°C.

Our results indicate that photoinhibition at low, non-freezing temperatures occurs via the same sequence of events we have earlier proposed to occur during photoinhibition under both anaerobic or aerobic conditions at room temperature [23,30]. Initially, all available plastoquinone is reduced [31] and Q_A^- is

TABLE I

Approximate half-times for inactivation of PS II activities, release of Mn and triggering of the D_1-protein during illumination of PS II membranes at 0–4°C and after a subsequent period at 20°C in the dark

	During illumination at 0 °C	During 2 h dark-incubation at 20°C after the inhibition
F_v/F_m	1–1.5 h	No further change
$H_2O \rightarrow$ PPBQ	1–1.5 h	No further change
$H_2O \rightarrow$ DCPIP	1–1.5 h	No further change
DPC → DCPIP	1–1.5 h	No further change
Multiline signal	1–1.5 h	No further change
Q_A^--Fe^{2+} signal	1–1.5 h	No further change
Manganese	3–4 h	No further change
Pheo	3–4 h	No further change
Signal II_{slow}	3–4 h	20–30% loss of remaining signal
D_1-protein	> 10 h	Triggered protein lost within 1 h
Triggering of the D_1-protein	3–4 h	-

accumulated in the reaction centers [30]. Subsequently, recent results indicate that Q_A^- is stabilized through protonation and further reduction to the double reduced state [23,26] which inhibits electron-transfer via Q_A. In the present study, double-reduction of Q_A provides a useful explanation for the simultaneous decrease in PS II electron transport and loss of the Q_A^--signal (Table I). Moreover, it is consistent with the loss of the S_2-state multiline signal (which can only be formed in presence of functional Q_A) and the lowering of the F_v/F_m fluorescence ratio. Similar to the situation during room-temperature photoinhibition, the damage to the D_1-protein, in this study revealed as triggering of the D_1-protein for degradation, is a subsequent event to the inhibition of steady-state electron transfer (Table I).

PS II reaction centers with double-reduced Q_A have been shown to form chlorophyll triplets during illumination [22,23]. In the absence of oxygen the chlorophyll triplets are essentially harmless but when oxygen is present, as in our experiments, chlorophyll triplets are known to react readily with oxygen to form singlet oxygen [32]. This toxic oxygen species is highly reactive and it has been proposed to damage the D_1-protein irreversibly [23,33] probably by reactions in the immediate vicinity of P680, thereby inactivating pigments, nearby redox-components or amino acids.

Simultaneously with the triggering of the D_1-protein, Tyr_D^+ and the primary charge separation reaction are lost (Table I; Scheme I). The lack of ^{3}P680 formation in our experiments can be explained since ^{3}P680 forming centers formed during the photoinhibition would be rapidly and irreversibly inactivated in the charge separation reaction by singlet oxygen. This is also consistent with the small, but significant, increase of reversible F_0 during the initial stages of photoinhibition (not shown). The increased [25,26], reversible F_0 was shown to originate from triplet forming centers with stabilized Q_A [23]. Under anaerobic conditions [23,25,26] such centers are built up continuously leading to a high F_0-level. However, under aerobic conditions this fraction is always small [26], most likely due to the irreversible reaction of these centers with singlet oxygen.

Our earlier experiments were performed at room-temperature and the damage to the D_1-protein and inactivation of the reaction center revealed itself as degradation of the protein [15,23]. At lower temperatures, however, the damaged D_1-protein is not proteolysed although it is triggered for degradation. In fact we were able to follow the kinetics for the formation of this earlier hypothetical triggered state (Scheme I). This was done by determining the fraction of degradable D_1 protein when, after various periods of illumination at low temperature, the samples were transferred to room-temperature (Fig. 1). The actual protein degradation was independent of light. Thus, the light-reactions involved only lead to the formation of the triggered state of the protein and it now seems clear that this is caused by oxidative damage induced by singlet oxygen. However, it is not clear how the

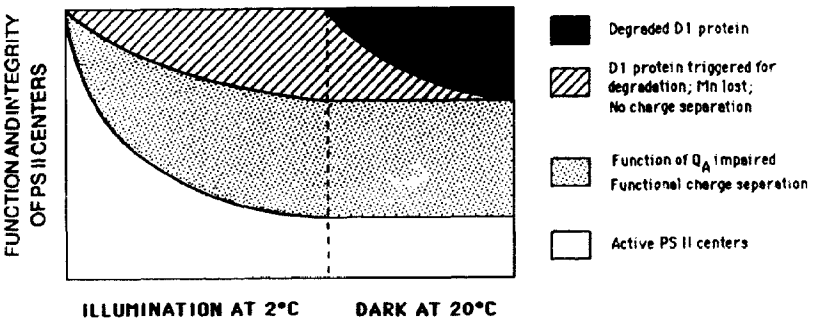

Scheme I.

D_1-protein is affected at the molecular level. Most likely, the light-dependent triggering is accompanied by a gross conformational change on the D_1-protein. This turns it into a substrate for a proteinase which is located within the PS II complex [7,8]. The conformational change of the D_1-protein is supported by the loss of Mn which occurs in parallel with the D_1-protein triggering rather than the actual degradation. This may also be consistent with the appearance of a modified form of the D_1 protein with altered electrophoretic migration during photoinhibition in vivo [34,35]. Moreover, our experiments were performed in a purified PS II preparation in the absence of added ATP which indicates that protein phosphorylation is not required for the triggering reactions.

In addition to these reactions that occur in the dominating fraction of centers, there are indications of an early partial inactivation on the donor side of PS II in agreement with Ref. 36. Here, we have observed that the decrease in inducible Q_A^- corresponded to the inhibition of the electron transport from DPC to DCIP. This is reasonable and shows that the essential block in the electron transfer occurs on the acceptor side in PS II. However, electron transport in absence of the artificial electron donor was inhibited somewhat faster (Fig. 2). This difference suggests that, in a minor fraction of centers, some early inhibition occurred at the donor side of PS II, but at present we cannot decide at which electron transfer step the inhibition occurred. Interestingly, it was recently shown that inhibition of protoplasts at 4°C is mainly caused by an oxygen-dependent mechanism, but that some oxygen-independent inhibition took place simultaneously [37].

Moreover, we observed that a stable cationic radical was induced during the illumination. The kinetics for the induction of this radical approximately correlated with the inactivation of the donor side measured by the difference in electron transport in presence and absence of the exogenous electron donor DPC. This supports the hypothesis that this radical was induced in the small fraction of centers which were able to reduce Q_A but had impaired or inefficient electron donation from the oxygen evolving system. During illumination these centers will perform stable charge separations. However, the electron hole on $P680^+$ or Tyr_Z^+ cannot be filled by donation from the normal donor, the oxygen evolving system. Instead, redox-components in the vicinity would donate an electron and become oxidized [38–40]. The radical linewidth and g-value did not correspond to the chlorophyll cation induced by 77 K illumination (9–10 Gauss, $g = 2.0025–2.0026$). In our view, one likely candidate for the radical is a carotenoid cation and in this context it is relevant that oxidation of carotenoids has been observed as a consequence of photoinhibition of PS II with impaired function of the donor side in absorbtion spectroscopy studies [41,42]. In addition, Blubaugh and coworkers [43] have observed the build up of a radical with a featureless radical EPR spectrum during photoinhibition of PS II lacking the Mn-cluster involved in the oxidation of water. This spectrum was tentatively assigned to a carotenoid cation but at present it is not clear that their spectrum represents the same species as our radical. Therefore, other possibilities than a carotenoid, like a modified tyrosine-radical or another oxidized aminoacid residue (for example a histidine [44]), cannot be excluded and final identification of our radical has to await further experimentation.

Acknowledgements

This study was supported by the Swedish Natural Science Research Council, the Carl Trygger Foundation and the Hasselblad foundation. K.J.v.W. was supported by the Foundation for Fundamental Biological Research, which is subsidised by the Netherlands Organization for the Advancement of pure Research. We gratefully acknowledge discussions with H. Salter, T. Hundal, I. Vass, I. Virgin and the technical help given by A.M. Tomka and T. Astlind. The EPR spectrometer was generously made available by Prof. A. Ehrenberg. Antibodies were generously supplied by Drs. I. Ohad and W. Vermaas.

References

1 Powles, S.B. (1984) Annu. Rev. Plant Physiol. 35, 15–44.
2 Kyle, D.J., Osmond, C.B. and Arntzen, C.J. (1987) Photoinhibition, Topics in Photosynthesis (Barber, J., ed.), Vol. 9, Elsevier, Amsterdam.
3 Krause, G.H. (1988) Physiol. Plant. 74, 566–609.
4 Andersson, B. and Styring, S. (1991) Curr. Top. Bioenerg. 16, 1–81.
5 Virgin, I., Ghanotakis, D.F. and Andersson, B. (1990) FEBS Lett. 269, 45–48.
6 Shipton, C.A. and Barber, J. (1991) Proc. Natl. Acad. Sci. USA 88, 6691–6695.
7 Virgin, I., Salter, A.H., Ghanothakis, D.F. and Andersson, B. (1991) FEBS Lett., 287, 125–128.
8 Shipton, C.A. and Barber, J. (1992) Biochim Biophys. Acta, in press.
9 Aro, E.-M., Hundal, T., Carlberg, I. and Andersson, B. (1990) Biochim. Biophys. Acta 1019, 269–275.
10 Berthold, D.A., Babcock, G.T. and Yocum, C.F. (1981) FEBS Lett. 134, 231–234.
11 Franzén, L.-G., Hansson, Ö. and Andréasson, L.E. (1985) Biochim. Biophys. Acta 808, 171–179.
12 Schreiber, U., Schliwa, U. and Bilger, W. (1986) Photosynth. Res. 10, 51–62.
13 Vermaas, W.F.J. and Rutherford, A.W. (1984) FEBS Lett. 175, 243–248.
14 Klimov, V.V., Dolan, E. and Ke, B. (1980) FEBS Lett. 112, 97–100.
15 Virgin, I., Styring, S. and Andersson, B. (1988) FEBS Lett. 233, 408–412.
16 Towbin, H., Staehelin, T. and Gordon, J. (1979) Proc. Natl. Acad. Sci. USA, 4350–4354.

17 Arnon, D.I. (1948) Plant Physiol. 24, 1–15.
18 Miller, A.-F. and Brudvig, G.W. (1991) Biochim. Biophys. Acta 1056, 1–18.
19 Debus, R.J., Barry, B.A., Babcock, G.T. and McIntosh, L. (1988) Proc. Natl. Acad. Sci. USA 85, 427–430.
20 Vermaas, W.F.J., Rutherford, A.W. and Hansson, Ö. (1988) Proc. Natl. Acad. Sci. USA 85, 8477–8481.
21 Butler, W.F., Calvo, R., Fredkin, D.R., Isaacson, R.A., Okamura, M.Y. and Feher, G. (1984) Biophys. J. 45, 947–973.
22 Van Mieghem, F.J.E., Nitschke, W., Mathis, P. and Rutherford, A.W. (1989) Biochim. Biophys. Acta 977, 207–214.
23 Vass, I., Styring, S., Hundal, T., Koivuniemi, A., Aro, E.-M. and Andersson, B. (1992) Proc. Natl. Acad. Sci. USA, 89, 1408–1412.
24 Okamura, M.Y., Satoh, K., Isaacson, R.A. and Feher, G. (1987) in Progress in Photosynthesis Research (Biggins, J., ed.), Vol. I, pp. 379–381, Martinus Nijhoff, Dordrecht.
25 Kirilovsky, D., Vernotte, C. and Etienne, A.-L. (1990) Biochemistry 29, 8100–8106.
26 Setlik, I., Allakhverdiev, S.I., Nedbal, L., Setlikova, E. and Klimov, V.V. (1990) Photosynth. Res. 23, 39–48.
27 Krause, G.H., Somersalo, S., Zumbusch, E., Weyers, B. and Laasch, H. (1990) J. Plant Physiol. 136, 472–479.
28 Hundal, T., Virgin, I., Styring, S. and Andersson, B. (1990) Biochim. Biophys. Acta 1017, 235–241.
29 Styring, S. and Rutherford, A.W. (1987) Biochemistry 26, 2401–2405.
30 Styring, S., Virgin, I., Ehrenberg, A. and Andersson, B. (1990) Biochim. Biophys. Acta 1015, 269–278.
31 Ohad, I., Koike, H., Shochat, S. and Inoue, Y. (1988) Biochim. Biophys. Acta 933, 288–298.
32 Asada, K. and Takahashi, M. (1987) in Topics in Photosynthesis (Barber, J., ed.), Vol. 9, pp. 227–288, Elsevier, Amsterdam.
33 Barber, J. (1990) in Current Research in Photosynthesis (Baltscheffsky, M., ed.) Vol. II, pp. 715–724, Kluwer, Dordrecht.
34 Callahan, F.E., Ghirardi, M.L., Sopory, S.K., Mehta, A.M., Edelman, M. and Mattoo, A.K. (1990) J. Biol. Chem. 265, 15357–15360.
35 Kettunen, R., Tyystjärvi, E. and Aro, E.-M. (1991) FEBS Lett. 290, 153–156.
36 Eckert, H.-J., Geiken, B., Bernarding, J., Napiwotzki, A., Eichler, H.-J. and Renger, G. (1991) Photosynth. Res. 27, 97–108.
37 Van Wijk, K.J. and Krause, G.H. (1991) Planta, in press.
38 Thompson, L.-M. and Brudvig, G.W. (1988) Biochemistry 27, 6653–6658.
39 Jegerschöld, C., Virgin, I. and Styring, S. (1990) Biochemistry 29, 6179–6186.
40 Barber, J. and Andersson, B. (1992) Trends Biochem. Sci., 17, 61–66.
41 Klimov, V.V., Shafiev, M.A. and Allakverdiev, S.I. (1990) Photosynth. Res. 23, 59–65.
42 Telfer, A., De Las Rivas, J. and Barber, J. (1991) Biochim. Biophys. Acta 1060, 106–114.
43 Blubaugh, D.J., Atamian, M., Babcock, G.T., Golbeck, J.H. and Cheniae, G.M. (1991) Biochemistry 30, 7586–7597.
44 Boussac, A., Zimmerman, J.-L., Rutherford, A.W. and Lavergne, J. (1990) Nature 347, 303–306.